Annals of Nuclear Medicine (2020) 34:549–558
https://doi.org/10.1007/s12149-020-01488-1

ORIGINAL ARTICLE

Diagnostic performance of whole-body bone scintigraphy in combination with SPECT/CT for detection of bone metastases

Yiqiu Zhang[1,2,3] · Beilei Li[1,2,3] · Bing Wu[1,2,3] · Haojun Yu[1,2,3] · Junyi Song · Yan Xiu[1,2,3] · Hongcheng Shi[1,2,3]

Received: 24 February 2020 / Accepted: 26 May 2020 / Published online: 24 June 2020

Abstract

Objective This retrospective study investigated the performance of whole-body bone scintigraphy combined with SPECT/CT and established a grading diagnostic criterion for bone metastases.

Methods We summarized signs of whole-body bone imaging combined with SPECT in nuclear medicine and CT signs of corresponding parts. Then we established a diagnostic criterion for bone metastases by using whole-body bone scintigraphy combined with local SPECT/CT. The criterion is classified into five grades. 120 patients with a total of 141 lesions underwent whole-body bone scintigraphy and SPECT/CT. Two reviewers read the images according to the diagnostic criterion. With pathological diagnosis as the "gold standard", the diagnostic efficacy for bone metastases and the diagnostic agreement between the two reviewers were analyzed to validate the feasibility of the criterion. Diagnostic effectiveness was expressed in terms of sensitivity, specificity, positive predictive value, negative predictive value, and accuracy.

Results The diagnostic accuracy of the two reviewers was 90.1% and 92.9% respectively, sensitivity was both 100%, specificity was 41.7% and 58.3%, positive predictive value was 89.3% and 92.1%, and negative predictive value was both 100%. The kappa value of the diagnostic tests performed by the two reviewers on whole-body bone scintigraphy combined with SPECT/CT was 0.919 ($P < 0.001$).

Conclusion The grading diagnostic criterion for bone metastases by whole-body bone scintigraphy combined with SPECT/CT has high diagnostic accuracy and good consistency between reviewers, but the specificity was still low even with SPECT/CT.

Keywords SPECT/CT · Malignant tumor · Diagnostic · Bone metastases

Introduction

99mTc-MDP whole-body bone scintigraphy is the most common method for diagnosing bone metastasis of malignant tumors. It mainly reflects information on bone blood flow and metabolism, and in this way detects whether there is tumor metastasis in the whole-body bone [1–4]. Compared with other imaging methods, it has good diagnostic efficiency. Local SPECT/CT imaging based on whole-body bone scintigraphy can not only confirm the osteolytic or osteogenic changes of bone metastasis, but also effectively identify bone degenerative lesions, fractures and other primary benign bone lesions. Compared with whole-body bone scintigraphy and SPECT, the accuracy of the diagnosis of tumor bone metastasis is improved [5–22]. The combination of whole-body bone scintigraphy and local SPECT/CT is the most succinct one-stop method for screening and diagnosing tumor bone metastasis. Although SPECT/CT has been widely used in the diagnosis of tumor bone metastasis, there is still a lack of uniform diagnostic criteria for total bone imaging and local SPECT/CT examination for bone metastasis.

This retrospective study followed cases that underwent SPECT/CT with equivocal skeletal lesions detected by whole-body bone scintigraphy in the past 10 years since the

Yiqiu Zhang and Beilei Li contributed equally to this work.

✉ Hongcheng Shi
shihongcheng163@163.com

[1] Department of Nuclear Medicine, Zhongshan Hospital, Fudan University, Shanghai 200032, China

[2] Nuclear Medicine Institute of Fudan University, Shanghai 200032, China

[3] Shanghai Institute of Medical Imaging, Shanghai 200032, China

introduction of SPECT/CT in the Department of Nuclear Medicine, Zhongshan Hospital, Fudan University. The final diagnosis of each skeletal lesion was based on pathological confirmation after biopsy or surgery within 4 weeks. Firstly, we obtained the data of bone metastasis and analyzed the characteristics of whole-body bone scintigraphy and SPECT/CT of bone metastases, summarized the whole-body bone scintigraphy combined with SPECT signs and CT signs, and established a grading diagnostic criterion for bone metastases by whole-body bone scintigraphy combined with SPECT/CT. Then we used this standard to independently read the whole-body bone scintigraphy images and SPECT/CT fusion images by two reviewers, with the pathological diagnosis considered as the "gold standard", with the diagnostic efficacy of the bone metastases and the diagnostic consistency between the two reviewers analyzed to verify the criterion.

Materials and methods

Patients

From April 2008 to November 2017, 43,717 patients underwent bone scintigraphy. Of them, 24,720 patients underwent SPECT/CT with equivocal skeletal lesions in the Department of Nuclear Medicine, Zhongshan Hospital, Fudan University. This study was approved by the Institutional Review Board of Zhongshan Hospital, Fudan University. All patients provided written informed consent prior to enrollment in the study.

Case inclusion criteria and exclusion criteria

Inclusion criteria

At least one of the positive skeletal lesions found in the range of SPECT/CT imaging was diagnosed by biopsy or surgery. All of the lesions included in the study were confirmed by pathological diagnosis.

Exclusion criteria

The patient had no history of malignant tumors, furthermore the pathological diagnosis of positive lesions in SPECT/CT was not a bone metastasis; the previous pathology was clearly diagnosed as a history of primary bone tumor or tumor bone metastasis; previous imaging studies diagnosed tumor bone metastases for which therapeutic intervention was given; the lesion site has a clear surgery history of primary bone tumor or other bone lesions.

Selected cases

A total of 120 patients were included (Table 1). Of them, 97 cases had a history of malignant tumors before bone scintigraphy (24 hepatocellular carcinoma; 22 lung cancer; 12 breast cancer; 12 colorectal cancer; 6 kidney cancer; 4 thyroid cancer; 3 esophageal cancer; 3 prostate cancer; 2 bladder cancer; nasopharyngeal carcinoma, lung cancer with nasopharyngeal carcinoma, gastric cancer, scalp squamous cell carcinoma, endometrial cancer, pancreatic cancer, retroperitoneal malignant pheochromocytoma, brain malignant glioma, and nasal rhabdomyosarcoma, one each), confirmed as bone metastases, primary bone tumors or other bone lesions by bone pathology; another 23 cases had no history of malignant tumors before bone scintigraphy confirmed as tumor bone metastasis (2 hepatocellular carcinoma; 6 lung cancer; 3 prostate cancer; breast cancer, kidney cancer, thyroid cancer, cholangiocarcinoma, and thymic carcinoma one each; 7 with bone metastases with unclear primary sites).

Bone scintigraphy

Whole-body planar scintigraphy was performed approximately 3 to 6 h after intravenous injection of approximately 1110 MBq (30 mCi) Tc-99m-MDP with a three-detector gamma camera (Prism-IRIX, Marconi Medical

Table 1 Types and numbers of primary tumors in 120 cases

Primary tumors	No. of patients (%)
Hepatocellular carcinoma	26 (21.7%)
Lung cancer	28 (23.3%)
Breast cancer	13 (10.8%)
Colorectal cancer	12 (10.0%)
Kidney cancer	7 (5.8%)
Prostate cancer	6 (5.0%)
Thyroid cancer	5 (4.2%)
Esophageal cancer	3 (2.5%)
Bladder cancer	2 (1.7%)
Nasopharyngeal carcinoma	1 (0.8%)
Nasopharyngeal carcinoma with lung cancer	1 (0.8%)
Gastric cancer	1 (0.8%)
Cholangiocarcinoma	1 (0.8%)
Thymic cancer	1 (0.8%)
Scalp squamous cell carcinoma	1 (0.8%)
Endometrial cancer	1 (0.8%)
Pancreatic cancer	1 (0.8%)
Retroperitoneal malignant pheochromocytoma	1 (0.8%)
Brain malignant glioma	1 (0.8%)
Nasal rhabdomyosarcoma	1 (0.8%)
Other cancers with unclear primary sites	7 (5.8%)

Systems, Cleveland, OH, USA) or two-detector gamma camera [Philips Precedence with 16-slice diagnostic CT (Philips, Medical System, Bothell, WI, USA) or Symbia Intevo with 16-slice diagnostic CT (Siemens Healthcare Ltd, Germany)] equipped with a low-energy, high-resolution, parallel-hole collimator. For planar whole-body scintigraphy acquisition, counts from the 20% energy windows at 140 keV were acquired in a 256 × 1024 matrix.

SPECT/spiral CT

Based on the findings of undetermined foci from planar whole-body scintigraphy, the patients underwent SPECT/CT scanning. Each SPECT/CT scan was acquired with the undetermined foci included in the center of the field of view. For SPECT acquisition, counts from the 15% energy window at 140 keV were acquired in a 64 × 64 matrix. A CT scan with the same field of view as the SPECT scan was acquired. The SPECT raw data were reconstructed into transaxial, coronal, and sagittal slices using reconstruction software (Astonish: Philips San Jose, CA, USA or Symbia: Siemens Healthcare Ltd, Germany). For all fused images, the accuracy of the matching of internal anatomic landmarks visible on both CT and SPECT was checked. Both SPECT and CT were performed with the patients stably lying supine and breathing shallowly. No misregistration exceeding 2 mm was found.

Analysis of characteristics of bone metastases

A total of 117 bone metastases were obtained from 100 patients with tumor bone metastasis. 60.7% (71/117) of lesions in the spine (including cervical, thoracic, and lumbar spine), 8.5% (10/117) in the thorax (including rib, clavicle, sternum, and scapula), 18.8% (22/117) in the pelvis (including hip, sacrum, and sacral iliac area), and 12.0% (14/117) in the limbs.

Whole-body bone scintigraphy and SPECT of 117 bone metastases showed 33.3% (39/117) for radioactive concentration in three or more sites except for the symmetrical part of the extremities, 1.7% (2/117) for 'doughnut sign' radioactive concentration, and 65.0% (76/117) for focal radioactive concentrated foci (49 cases of spinal lesions located in the pedicle and vertebral body, 2 cases of rib lesions elongated along the ribs, 25 cases located in other parts).

CT imaging of 117 bone metastases showed 6.0% (7/117) for osteogenic bone destruction, 16.2% (19/117) for mixed bone destruction, and 77.8% (91/117) for osteolytic bone destruction (including 29 cases with soft tissue masses and 24 cases with pathological fractures).

Establishment of whole-body bone scintigraphy combined with SPECT sign classification in nuclear medicine and CT sign classification

According to the characteristics of the above bone metastases and related literature [18–22] on the diagnosis of tumor bone metastasis by whole-body bone scintigraphy and SPECT/CT imaging, we summarized the signs of whole-body bone scintigraphy combined with SPECT in nuclear medicine and CT signs of corresponding parts.

Signs of whole-body bone scintigraphy combined with SPECT

The signs are: (1) "double track sign" and "string beads sign", the concentration of joints in the limbs, chest, costal and sacroiliac, the concentration of borderline junction of sternum, and the radioactive sparsity of corresponding bones in radiotherapy areas; (2) focal radioactivity concentration or sparsity; (2A) spinal lesions adjacent to the edge of the vertebral body or protruding outside the outline of the vertebral body and vertebral facet joints, rib lesions being round, quasi-circular or short strip, but vertical to the long axis of the ribs; lesions of the metaphyseal of the long bone involving the articular surface; (2B) spinal lesions located within the vertebral body and pedicles, and rib lesions elongated along the ribs; (3) radioactivity concentration of three or more sites except for symmetrical sites of the limbs; (4) "doughnut sign" and "super scintigraphy".

CT signs of the corresponding parts

The signs are: (1) degenerative changes such as hyperosteogeny, osteosclerosis, Schmorl's node, bone island, compression of vertebrae, non-pathological fracture, increased or decreased bone density with clear focus in bone boundary, and intramedullary bone density changes unassociated with cortical bone destruction; (2) osteogenic bone destruction; (3) mixed bone destruction; 4, osteolytic bone destruction; (4A) osteolytic destruction of the spine invading intervertebral disc, or bone destruction of the metaphyseal of the long bone involving the articular surface with or without dead bone formation; (4B) associated with soft tissue masses; (4C) associated with pathological fractures.

Then we established the diagnostic criterion for bone metastases using whole-body bone scintigraphy combined with local SPECT/CT. The grading diagnostic criterion is classified into five grades (Table 2).

Image analyses

All images were independently interpreted by two experienced nuclear medicine physicians who have both CT and

Table 2 The grading diagnostic criterion for bone metastases using whole-body bone scintigraphy combined with local SPECT/CT

Grade	Diagnosis	Nuclear medicine signs	CT signs
1	Benign	1, 2, 2A, 2B	1
2	Likely benign	2A	4A
3	Likely bone metastases	2	2, 3, 4, 4B, 4C
4	Highly likely bone metastases	2B	2, 3, 4, 4B, 4C
5	Bone metastases	3, 4	2, 3, 4, 4B, 4C

nuclear medicine physician qualifications and did not participate in the summary or analysis of the characteristics of the above-mentioned bone metastasis lesions. The reviewers were aware of the patients' gender, age, any history of histologically confirmed extraskeletal malignancy and its location and type, but unaware of the results of other imaging modalities and laboratory tests. Two reviewers read the images separately according to the diagnostic criterion.

Each reviewer performed a separate reading of the whole-body bone image and SPECT/CT fusion image on the display of each workstation. According to the criterion proposed in this study, the lesions were judged as benign (Grade 1), likely benign (Grade 2), likely bone metastasis (Grade 3), highly likely bone metastasis (Grade 4), and bone metastasis (Grade 5).

Statistical analysis

The data were computed using SPSS 22.0 software (SPSS Inc., Chicago, IL, USA). With pathological diagnosis as the "gold standard", the diagnostic efficacy of bone metastases and the diagnostic consistency between the two reviewers were analyzed to verify the feasibility of the criterion. Grade 1 and grade 2 were classified as non-tumor bone metastases, while grade 3, grade 4, and grade 5 were classified as tumor bone metastases. Diagnostic effectiveness was expressed in terms of sensitivity, specificity, positive predictive value, negative predictive value, and accuracy. The consistency between observers was evaluated by the Kappa test. The kappa values ranged from − 1 (complete disagreement) to + 1 (perfect agreement). Kappa scores were classified as follows: 0, chance agreement; < 0.20, poor agreement; 0.21–0.40, fair agreement; 0.41–0.60, moderate agreement; 0.61–0.80, substantial agreement; and 0.81–1.00, almost perfect agreement [10]. $P < 0.05$ was considered statistically significant.

Results

Pathological diagnosis of all lesions

A total of 141 lesions in 120 cases were pathologically diagnosed. There were 117 bone metastases in 100 patients with bone metastases, 21 benign bone lesions in 17 patients, 2 patients had single primary malignant bone tumor lesions, and 1 patient had a single primary bone tumor intermediate lesion (Table 3).

Diagnostic efficacy of whole-body bone scintigraphy combined with SPECT/CT between two reviewers

Two reviewers analyzed the results of grading diagnosis and pathological diagnosis of the whole-body bone scintigraphy combined with SPECT/CT (Table 4). With the pathological diagnosis considered as the "gold standard", the diagnosis of whole-body bone scintigraphy combined with SPECT/CT is benign (grade 1), possibly benign (grade 2) classified as non-tumor bone metastasis, likely bone metastasis (grade 3), highly likely bone metastasis (grade 4), and bone metastasis (grade 5) classified as tumor bone metastasis. The accuracy of the diagnosis of the two reviewers was 90.1% and 92.9%, respectively, sensitivity was both 100%, specificity was 41.7% and 58.3%, respectively, positive predictive value was 89.3% and 92.1%, respectively, and negative predictive value was both 100%.

Consistency evaluation of graded diagnosis between two reviewers

The distribution of grading diagnosis results of 141 lesions by whole-body imaging and SPECT/CT of the two reviewers is shown in Table 5. The κ value of the two reviewers' whole-body bone imaging combined with SPECT/CT grading diagnostic consistency test was 0.919 ($P < 0.001$), indicating that the consistency of the two reviewers was very high using this method.

The cases of inconsistent diagnosis between the two reviewers or inconsistent with pathological diagnosis

There were 17 lesions in 14 patients inconsistent between the two reviewers or inconsistent with pathological diagnosis (Table 6). Because the signs of SPECT and CT are not specific, 12 benign skeletal lesions in ten patients with malignant tumors were misdiagnosed as metastasis, likely

Table 3 Pathological diagnosis of 141 lesions in 100 patients

Lesion nature	No. of cases/lesions	Pathological diagnosis	No. of cases/lesions
Bone metastases	100/117	Metastasis from hepatocellular carcinoma	25/26
		Metastasis from lung cancer	26/31
		Metastasis from breast cancer	10/14
		Metastasis from colorectal cancer	7/7
		Metastasis from kidney cancer	7/8
		Metastasis from prostate cancer	6/8
		Metastasis from thyroid caner	3/5
		Metastasis from esophageal cancer	1/1
		Metastasis from bladder cancer	1/1
		Metastasis from nasopharyngeal cancer	2/3
		Metastasis from gastric cancer	1/1
		Metastasis from cholangiocarcinoma	1/2
		Metastasis from thymic caner	1/1
		Metastasis from retroperitoneal Malignant pheochromocytoma	1/1
		Metastasis from rhabdomyosarcoma	1/1
		Metastasis from other cancers with Unclear primary sites	7/7
Non-bone metastases			
Benign lesion	17/21	Inflammation (including tuberculosis)	8/11 (2/3)
		Bone tissue hyperplasia, degeneration	6/7
		Hemangiolymphangioma	1/1
		Plasma cell proliferative lesion	1/1
		Osteonecrosis	1/1
Intermediate primary bone tumor	1/1	Langerhans cell histiocytosis	1/1
Malignant primary bone tumor	2/2	Osteosarcoma	1/1
		Plasmacytoma	1/1

Table 4 Comparison of diagnosis criterion of whole-body bone imaging combined with SPECT/CT and pathological diagnosis

Reviewers	Whole-body bone imaging combined with SPECT/CT		Pathological diagnosis		Bone metastases rate (%)
	Diagnosis criterion	No. of lesions	Bone metastases	Non-bone metastases	
Reviewer A	Grade 1	7	0	7	0
	Grade 2	3	0	3	0
	Grade 3	31	25	6	80.6
	Grade 4	58	51	7	87.9
	Grade 5	42	41	1	97.6
Reviewer B	Grade 1	10	0	10	0
	Grade 2	4	0	4	0
	Grade 3	29	25	4	86.2
	Grade 4	56	51	5	91.1
	Grade 5	42	41	1	97.6

metastasis or highly likely metastasis by at least one reviewer (cases 1–4 and cases 6–11 in Table 6), including five non-specific inflammatory lesions (cases 1–4 in Table 6, Fig. 1), three tuberculosis lesions (case 5 and case 6 in Table 6), one humerus bone tissue hyperplasia (case 8 in Table 6), one nucleus pulposus of lumbar degeneration (case 9 in Table 6), one thoracic vertebral lymphangioma (case 10 in Table 6), and one thoracic plasma cell proliferative lesion (case 11 in Table 6). A case of lumbar Langerhans cell histiocytosis in a patient with rectal cancer which showed osteolytic bone destruction on CT image and radioactive concentration located within the vertebral body and the pedicles on SPECT

Table 5 Distribution of diagnosis criterion results of whole-body bone imaging combined with SPECT/CT of two reviewers

	Reviewer A				
	Grade 1	Grade 2	Grade 3	Grade 4	Grade 5
Reviewer B					
Grade 1	7	Grade	1	0	0
Grade 2	0	0	2	2	0
Grade 3	0	1	28	0	0
Grade 4	0	0	0	56	0
Grade 5	0	0	0	0	42

image was misdiagnosed as highly probable bone metastasis by both reviewers (case 12 in Table 6, Fig. 2). A case of pubic osteosarcoma lesion in a patient with thyroid cancer which showed bone destruction on CT image and radioactive concentration located in the lesion on SPECT image was misdiagnosed as a likely bone metastasis by both reviewers (case 13 in Table 6). A case of thoracic plasmacytoma in a patient with colon cancer which showed bone destruction and vertebral compression on CT image and radioactive concentration located in the vertebral body and the pedicles on SPECT image was misdiagnosed as highly likely bone metastasis by both reviewers (case 14 in Table 6, Fig. 3). Two endplate inflammations of the lumbar spine in a patient with colon cancer were diagnosed as benign and possibly benign by both reviewers, respectively, and the results of the diagnosis were inconsistent (case 5 in Table 6).

Discussion

On the basis of bone planar imaging, the clinical application of SPECT/CT with diagnostic CT, through the anatomical and morphological diagnostic information provided by diagnostic CT images, achieves accurate anatomical position of lesions and improves the diagnostic accuracy of tumor bone metastasis.

Bone metastases can occur in any part of the body. The typical nuclear medicine images appear as multiple, scattered, varying in size, and different forms of radioactive accumulation. The most common sites are in the central axis bone such as the spine, ribs, and pelvis. For example,

Table 6 Cases with inconsistent diagnosis between two physicians and cases with inconsistent pathological diagnosis

No.	Sex	Age	Primary tumor	Lesion location	Reviewer A	Reviewer B	Pathological diagnosis
1	Male	53	Glioma	Femur	Likely benign	Likely bone metastases	Inflammation
2	Male	53	Scalp squamous cell carcinoma	Rib	Bone metastases	Bone metastases	Inflammation
3	Female	63	Breast cancer	Clavicle	Likely bone metastases	Likely bone metastases	Inflammation
4	Male	66	Bladder cancer	Lumbar spine	Highly likely bone metastases	Highly likely bone metastases	Inflammation
5	Male	71	Colorectal cancer	Lumbar spine	Highly likely bone metastases	Benign	Inflammation
				Lumbar spine	Highly likely bone metastases	Benign	Inflammation
6	Male	63	Esophageal cancer	Lumbar spine	Highly likely bone metastases	Highly likely bone metastases	Tuberculosis
7	Male	29	Pancreatic cancer	Shoulder blade	Likely bone metastases	Highly likely bone metastases	Tuberculosis
				Humerus	Likely bone metastases	Highly likely bone metastases	Tuberculosis
8	Female	32	Breast cancer	Humerus	Likely bone metastases	Benign	Bone tissue hyperplasia
9	Female	83	Rectal cancer	Lumbar spine	Highly likely bone metastases	Highly likely bone metastases	Degenerated nucleus pulposus
10	Male	42	Hepatocellular carcinoma	Thoracic spine	Highly likely bone metastases	Highly likely bone metastases	Hemangiolymphangioma
11	Male	65	Lung cancer	Thoracic spine	Likely bone metastases	Likely bone metastases	Plasma cell proliferative lesion
12	Male	70	Rectal cancer	Lumbar spine	Highly likely bone metastases	Highly likely bone metastases	Langerhans cell histiocytosis
13	Female	66	Thyroid cancer	Pubic	Likely bone metastases	Likely bone metastases	Osteosarcoma
14	Male	57	Colorectal cancer	Thoracic spine	Highly likely bone metastases	Highly likely bone metastases	Plasmacytoma

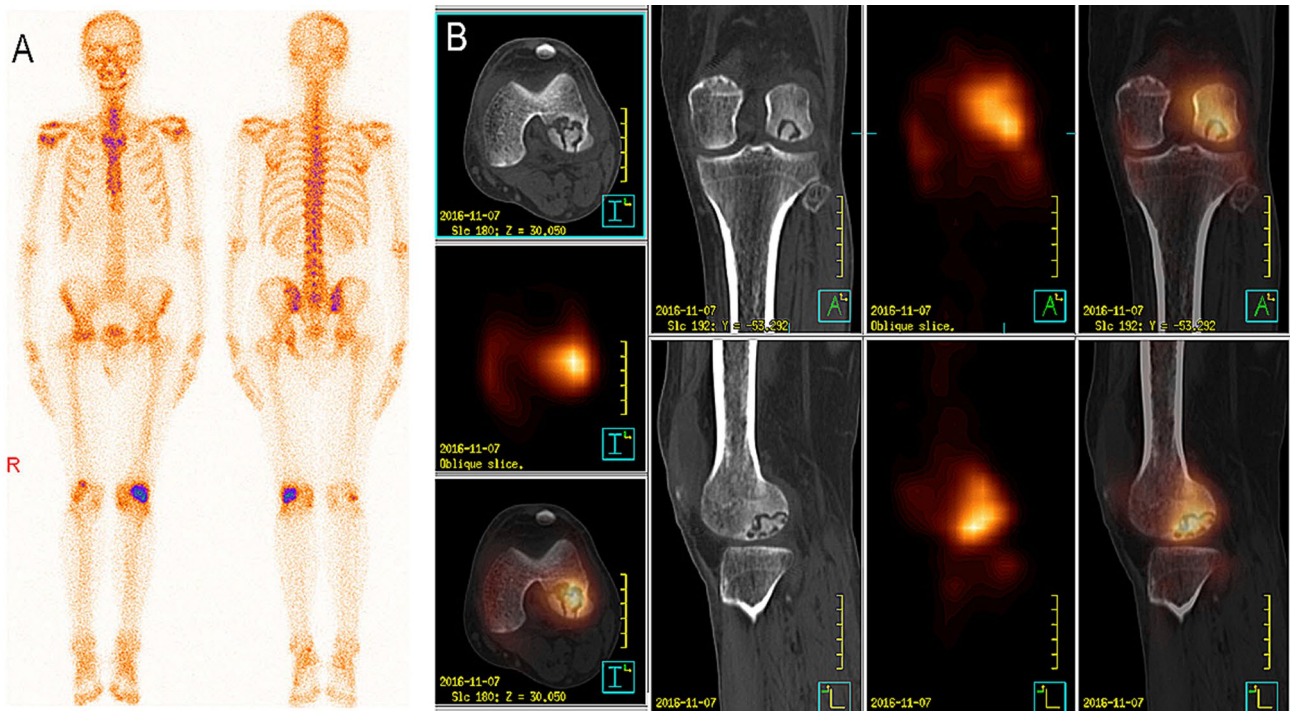

Fig. 1 Male, 53 years old, 7 months after cerebral glioma surgery, left knee pain without obvious cause for more than 1 month. Whole-body bone plane image shows abnormal radioactive concentration at the lower left femur (**a**). SPECT/CT image shows left lower femur bone destruction with abnormal radioactive concentration (**b**). Two reviewers diagnosed it as likely benign and likely bone metastases, respectively. The patient underwent left lower femoral lesion scraping and bone cement filling. The postoperative pathological diagnosis was inflammation

multiple asymmetric radioactive abnormalities throughout the body, radioactive abnormal distribution of ribs along the direction of the ribs or the involvement of the spine in the pedicle is considered to be a more reliable sign of metastasis. CT findings of tumor bone metastases are osteolytic, osteogenic or mixed bone destruction, which may be accompanied by soft tissue mass formation, pathological fractures, etc. Metastatic intertrabecular vertebral tumors that infiltrate the marrow space without trabecular bone alteration are not visible on CT or bone scintigraphy [23]. Some benign lesions also have some characteristic signs, such as "double track sign" and "bead sign" of whole-body imaging. Radioactive concentration of the limb joints, thoracic rib joint, acromioclavicular joint and sternal angle. Radioactive sparseness of bones within the radiotherapy area; the lesion of the spine is adjacent to the edge of the vertebral body of the intervertebral disc, protrudes beyond the contour of the vertebral body or at the facet joint of the vertebra. Rib lesions are round, oval, or short strips perpendicular to the long axis of the rib. On this basis, the classification of the whole-body bone scintigraphy and SPECT signs of skeletal lesions and the CT features of the corresponding sites were summarized. The grading diagnosis of tumor bone metastasis by whole-body bone scintigraphy combined with SPECT/CT was proposed. The diagnostic efficacy was verified in the study.

The kappa scores for the degree of agreement between the two reviewers using whole-body bone imaging combined with SPECT/CT grading diagnostic consistency test was 0.919 ($P < 0.001$), indicating that the consistency of the two reviewers was very good. Bone whole-body imaging and SPECT/CT imaging, under the same conditions of inspection equipment, collection conditions, image processing, etc., may lead to inconsistent diagnostic results because of differences in the level of clinical diagnosis between different reviewers and differences in the analysis of characteristics of different signs. In this study, the consistency between different reviewers using the same grading diagnostic criterion was very good, which indicated that there was no significant difference between the two reviewers for the whole-body bone imaging and SPECT signs and CT image recognition for grading diagnosis. Thus, the grading diagnostic criterion can minimize the difference in diagnostic results caused by inconsistent diagnostic levels of the reviewers.

The advantage of nuclear medicine is its high sensitivity and low specificity. Radioactive concentration may occur regardless of bone metastasis, primary bone tumor, inflammation, trauma, fracture, degenerative changes, etc. CT findings of bone metastases are osteolytic, osteogenic or mixed bone destruction, which may be accompanied by soft tissue

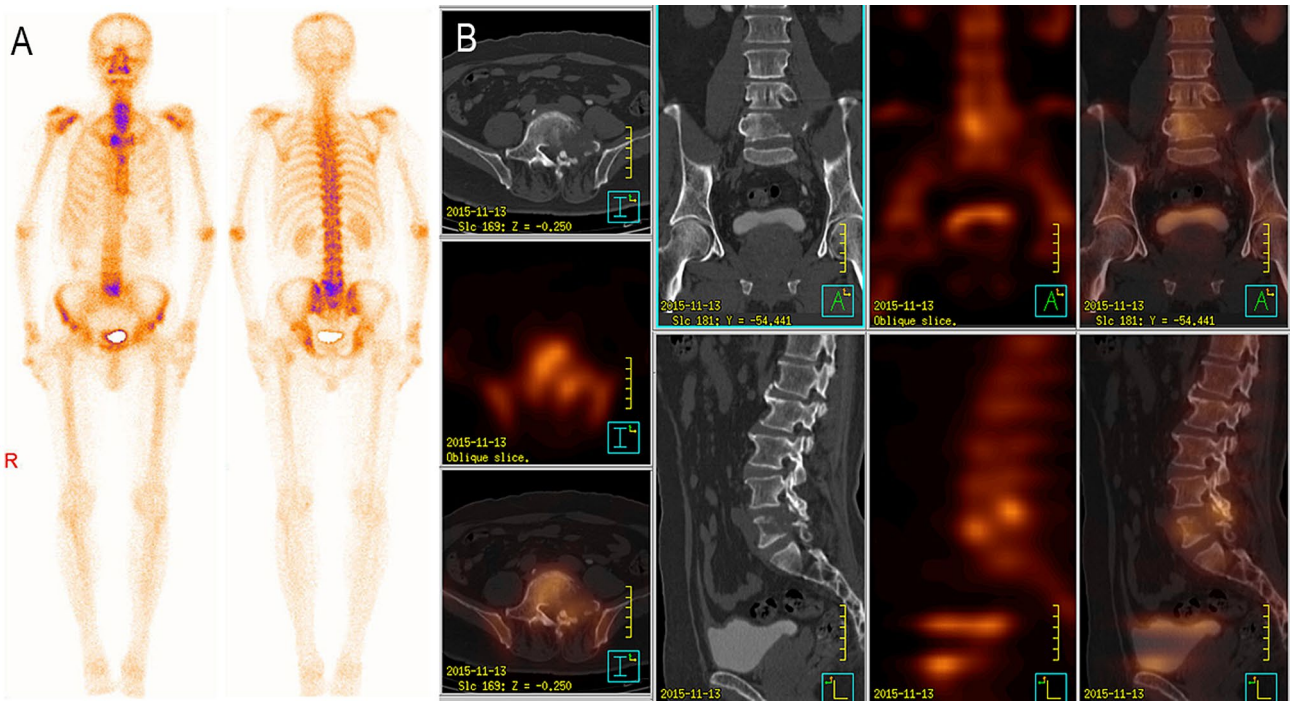

Fig. 2 Male, 70 years old, 7 years after rectal cancer surgery, low back pain with left lower extremity pain without obvious cause for more than 1 month. Whole-body bone plane image shows abnormal radioactive concentration at the fifth lumbar spine (**a**). SPECT/CT image shows fifth lumbar vertebral body and left accessory osteolytic bone destruction with abnormal radioactive concentration (**b**). Both reviewers diagnosed it as highly likely bone metastases. The patient underwent fifth lumbar spine tumor resection and internal fixation. The postoperative pathological diagnosis was Langerhans cell histiocytosis

mass formation, pathological fractures, etc. However, CT images of some bone inflammatory lesions or benign bone lesions can also manifest as bone destruction and pathological fractures. For example, some lesions of vertebral tuberculosis also manifest as osteolytic bone destruction involving the vertebral body or pedicle, and it is easy to be misdiagnosed as tumor bone metastasis when intervertebral disc invasion is not obvious. In this study, five non-specific inflammatory lesions in four patients with malignant tumors and three tuberculosis lesions in two patients were misdiagnosed as metastasis, highly likely metastasis or likely metastasis by at least one reviewer. Bone proliferative lesion of a breast cancer patient showed a soft tissue density in the medullary cavity with local radioactive concentration, which was misdiagnosed as likely metastasis by a reviewer. A Schmorl's nodule of the lumbar spine in an elderly patient with rectal cancer was misdiagnosed as highly likely metastasis by both reviewers. The thoracic hemangiolymphangioma of a liver cancer patient showed pathological fractures and was misdiagnosed as highly probable metastasis by both reviewers. The pathological fracture of thoracic vertebral hemangiolymphangioma after trauma was first considered to be bone metastasis due to the history of liver cancer. A thoracic plasma cell proliferative lesion of a lung cancer patient that showed osteolytic changes was misdiagnosed as likely metastasis by both reviewers. A lumbar Langerhans cell histiocytosis of a rectal cancer patient showed osteolytic bone destruction of vertebral bodies and pedicles with radioactive concentration, which was misdiagnosed as highly likely metastasis by both reviewers. A pubic osteosarcoma of a thyroid cancer patient showed bone destruction and soft tissue mass formation with radioactive concentration was misdiagnosed as likely metastasis by both reviewers. A single plasmacytoma of the thoracic spine of a colon cancer patient showed osteolytic bone destruction of the vertebral body and pedicle with peripheral osteogenic changes accompanied by radioactive concentration, which was misdiagnosed as highly likely metastasis by both reviewers. Langerhans cell histiocytosis, osteosarcoma and plasmacytoma belong to primary malignant bone tumor. Their nuclear medicine and CT signs lack specificity and can be expressed in varying degrees of bone destruction and radioactive concentration. Especially when patients have a history of malignant tumors, they are easily misdiagnosed as having bone metastasis. In addition, two endplate inflammations of the lumbar spine of a colon cancer patient were inconsistently diagnosed as benign and likely benign by the two reviewers.

When the manifestations of nuclear medicine and the CT morphological features of some benign lesions or primary bone tumors are atypical, especially in the case of bone

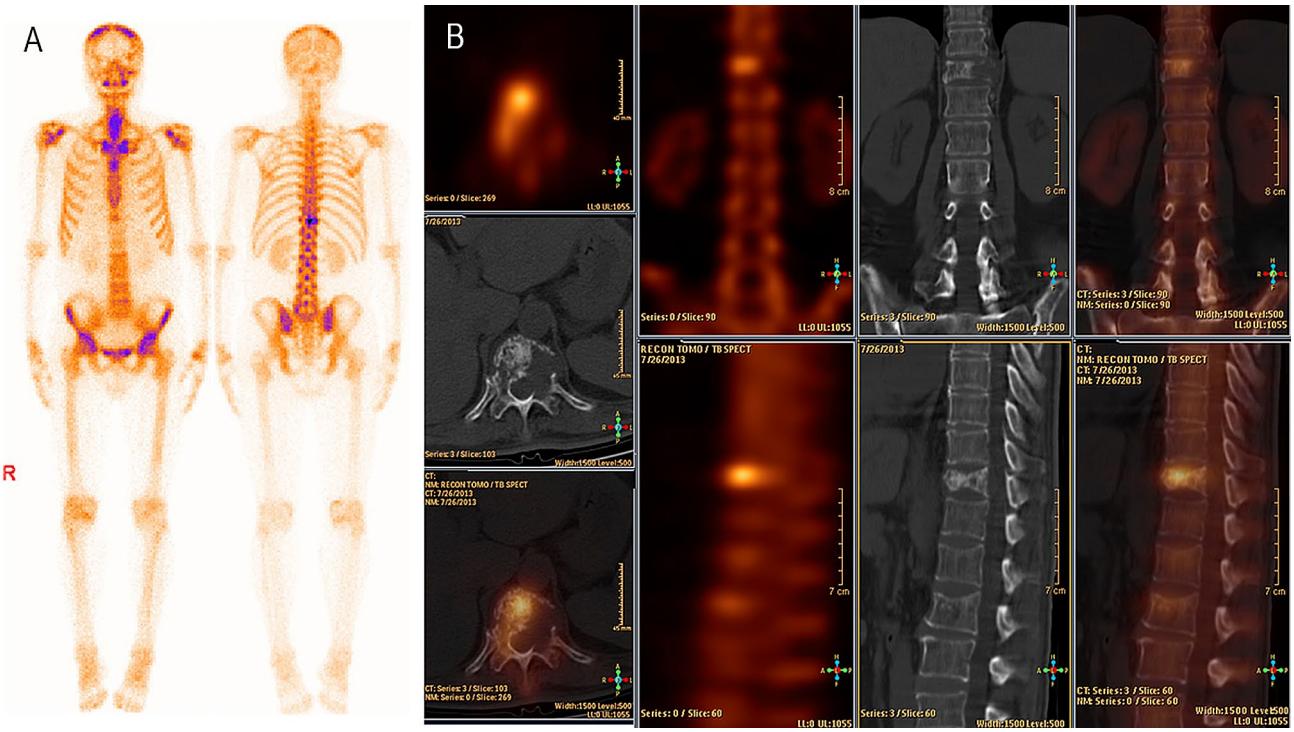

Fig. 3 Male, 57 years old, 10 years after colon cancer surgery, low back pain without obvious cause for 2 months. Whole-body bone plane image shows 11th thoracic abnormal radioactive concentration (**a**). SPECT/CT image shows 11th thoracic vertebral body and left accessory osteolytic bone destruction with abnormal radioactive concentration (**b**). Both reviewers diagnosed it as highly likely bone metastases. The patient underwent fifth lumbar vertebral tumor resection and internal fixation. The postoperative pathological diagnosis was plasmacytoma

destruction, it is still very difficult to identify bone metastases in patients with malignant tumors, and to a large extent it also depends on the clinical experience of the reviewers and the amount of medical history information and other related imaging data.

The 141 lesions in 120 patients included in this study were based on pathological diagnosis as the gold standard, making the data of this study more reliable. However, the current study has a few limitations. Many metastatic bone tumors and most benign bone lesions diagnosed by imaging are not recommended for surgical resection or biopsy, resulting in a limited number of cases included in the sample study. Moreover, due to the very small number of benign cases, most benign lesions obtained by pathological diagnosis are not well diagnosed by imaging or subjected to surgery until the bone lesion affects important functions or patient quality of life, introducing bias into the statistical data. Furthermore, these benign lesions did not reflect the proper population of benign lesions as encountered in clinics.

Conclusion

This study investigated the performance of SPECT/CT combined with whole-body bone scintigraphy and the diagnostic criterion for bone metastases to screen skeletal lesions in malignant tumor patients with high diagnostic accuracy and good consistency among different reviewers, but the specificity was still low even with SPECT/CT.

Acknowledgements This work was supported by the Scientific Research Program of Shanghai Municipal Commission of Health and Family Planning (Grant no. 201740201), the Shanghai Municipal Key Clinical Specialty (Grant no. shslczdzk03401) and the Technology Support Projects of Shanghai Science and Technology Committee (Grant no. 17411950300).

Compliance with ethical standards

Conflict of interest The authors declare no conflicts of interest.

References

1. Love C, Din AS, Tomas MB, Kalapparambath TP, Palestro CJ. Radionuclide bone imaging: an illustrative review. Radiographics. 2003;23:341–58.
2. Bellah RD, Summerville DA, Treves ST, Micheli LJ. Low back pain in adolescent athletes: detection of stress injury to the pars interarticularis with SPECT. Radiology. 1991;180:509–12.
3. Kobayashi K, Okuyama C, Kubota T, Nakai T, Ushijima Y, Nishimura T. Do short-time SPECT images of bone scintigraphy improve the diagnostic value in the evaluation of solitary lesions in the thoracic spine in patients with extraskeletal malignancies? Ann Nucl Med. 2005;19:557–66.
4. Rybak LD, Rosenthal DI. Radiological imaging for the diagnosis of bone metastases. Q J Nucl Med. 2001;45:53–64.
5. Zhao Z, Li L, Li F, Zhao L. Single photon emission computed tomography/spiral computed tomography fusion imaging for the diagnosis of bone metastasis in patients with known cancer. Skeletal Radiol. 2010;39:147–53.
6. Helyar V, Mohan HK, Barwick T, Livieratos L, Gnanasegaran G, Clarke SE. The added value of multislice SPECT/CT in patients with equivocal bony metastasis from carcinoma of the prostate. Eur J Nucl Med Mol Imaging. 2010;37:706–13.
7. Zhang Y, Shi H, Gu Y, Xiu Y, Li B, Zhu W. Differential diagnostic value of single-photon emission computed tomography/spiral computed tomography with Tc-99m-methylene diphosphonate in patients with spinal lesions. Nucl Med Commun. 2011;32:1194–200.
8. Sharma P, Singh H, Kumar R, Bal C, Thulkar S, Seenu V, et al. Bone scintigraphy in breast cancer: added value of hybrid SPECT-CT and its impact on patient management. Nucl Med Commun. 2012;33:139–47.
9. Zhang Y, Shi H, Cheng D, Jiang L, Xiu Y, Li B, et al. Added value of SPECT/spiral CT versus SPECT in diagnosing solitary spinal lesions in patients with extraskeletal malignancies. Nucl Med Commun. 2013;34:451–8.
10. Utsunomiya D, Shiraishi S, Imuta M, Tomiguchi S, Kawanaka K, Morishita S, et al. Added value of SPECT/CT fusion in assessing suspected bone metastasis: comparison with scintigraphy alone and nonfused scintigraphy and CT. Radiology. 2006;238:264–71.
11. Schillaci O, Danieli R, Manni C, Simonetti G. Is SPECT/CT with a hybrid camera useful to improve scintigraphic imaging interpretation? Nucl Med Commun. 2004;25:705–10.
12. Hamann M, Aldridge M, Dickson J, Endozo R, Lozhkin K, Hutton BF. Evaluation of a low-dose slow-rotating SPECT-CT system. Phys Med Biol. 2008;53:2495–508.
13. Strobel K, Burger C, Seifert B, Husarik DB, Soyka JD, Hany TF. Characterization of focal bone lesions in the axial skeleton: performance of planar bone scintigraphy compared with SPECT and SPECT fused with CT. Am J Roentgenol. 2007;188:W467–W474474.
14. Romer W, Nomayr A, Uder M, Bautz W, Kuwert T. SPECT-guided CT for evaluating foci of increased bone metabolism classified as indeterminate on SPECT in cancer patients. J Nucl Med. 2006;47:1102–6.
15. Iqbal B, Currie GM, Wheat JM, Raza H, Kiat H. The incremental value of SPECT/CT in characterizing solitary spine lesions. J Nucl Med Technol. 2011;39:201–7.
16. Horger M, Bares R. The role of single-photon emission computed tomography/computed tomography in benign and malignant bone disease. Semin Nucl Med. 2006;36:286–94.
17. Reinartz P, Schaffeldt J, Sabri O, Zimny M, Nowak B, Ostwald E, et al. Benign versus malignant osseous lesions in the lumbar vertebrae: differentiation by means of bone SPET. Eur J Nucl Med. 2000;27:721–6.
18. Zhang Y, Shi H, Li B, Cai L, Gu Y, Xiu Y. The added value of SPECT/spiral CT in patients with equivocal bony metastasis from hepatocellular carcinoma. Nuklearmedizin. 2015;54:255–61.
19. Lei J, Lei H, Tan H, Hu P, Zhang Y, Shi H. Diagnostic value of 99mTc-MDP SPECT/spiral CT in assessing indeterminate spinal solitary lesion of patients without malignant history. Ann Nucl Med. 2013;27:460–7.
20. Zhang Y, Shi H, Li B, Xiu Y, Cai L, Gu Y, et al. Diagnostic value of 99mTc-MDP SPECT/Spiral CT combined with three-phase bone scintigraphy in assessing suspected bone tumors in patients with no malignant history. Nucl Med Commun. 2015;36:686–94.
21. Zhang Y, Li B, Shi H, Yu H, Gu Y, Xiu Y. Added value of SPECT/spiral CT versus SPECT or CT alone in diagnosing solitary skeletal lesions. Nuklearmedizin. 2017;56:139–45.
22. Keidar Z, Israel O, Krausz Y. SPECT/CT in tumor imaging: technical aspects and clinical applications. Semin Nucl Med. 2003;33:205–18.
23. Yamaguchi T. Intertrabecular vertebral metastases: metastases only detectable on MR imaging. Semin Musculoskelet Radiol. 2001;5(2):171–5.